

Supporting Information

[ICl₄]⁻: A Large Anisotropic Planar Anion Group Produces Giant Birefringence

Yi-Chen Liu,^{ab} Ming-Zhi Zhang,^{ab} Chun-Li Hu^a, Jiang-Gao Mao^{*ab}

[a] Y.-C. Liu, M.-Z Zhang, C.-L. Hu, J.-G. Mao
State Key Laboratory of Functional Crystals and Devices, Fujian Institute of Research on the Structure of Matter
Chinese Academy of Sciences
Fuzhou, 350002, P. R. China
E-mail: mjpg@fjirsm.ac.cn

[b] Y.-C. Liu, M.-Z Zhang, C.-L. Hu, J.-G. Mao
University of Chinese Academy of Sciences
Beijing 100039, P. R. China

Table of Contents

Section	Page
Experimental Procedures	S3
Table S1. Crystallographic Data and Structure Refinement Details for $C_5H_7N_2Cl_4$.	S4
Table S2. Bond Lengths and Bond Angles for crystal $C_5H_7N_2Cl_4$.	S5
Table S3. Hydrogen Bond Lengths (Å) and Bond Angles (°) in $C_5H_7N_2Cl_4$.	S6
Table S4. Assignments of Additional Absorption Peaks in the IR Spectra of $C_5H_7N_2Cl_4$.	S6
Table S5. Comparisons of the Optical Property of Compound containing $[IO_3]^-$ group.	S7
Figure S1. The powder X-ray diffraction analysis of $C_5H_7N_2Cl_4$.	S8
Figure S2. The energy-dispersive X-ray spectroscopy of $C_5H_7N_2Cl_4$.	S8
Figure S3. The UV-vis-NIR diffuse reflectance spectra and experimental bandgap of $C_5H_7N_2Cl_4$.	S8
Figure S4. The infrared (IR) spectra of $C_5H_7N_2Cl_4$.	S9
Figure S5. TG and DSC curves of $C_5H_7N_2Cl_4$.	S9
Figure S6. (a) the original $C_5H_7N_2Cl_4$ under the cross-polarized light; (b) $C_5H_7N_2Cl_4$ achieving complete extinction; (c) the thickness of $C_5H_7N_2Cl_4$ used for birefringence measurement.	S9
Figure S7. Band structure of $C_5H_7N_2Cl_4$.	S10
Figure S8. PDOS and TDOS diagrams for $C_5H_7N_2Cl_4$.	S10
Figure S9. Distribution of the rotated ac plane and diagonalized dielectric tensor axes of $C_5H_7N_2Cl_4$.	S11
Figure S10. Refractive index and calculated birefringence of $C_5H_7N_2Cl_4$.	S11

Experimental Procedures

Synthesis.

4-Aminopyridine (99%), HIO₃ (99%), HCl (36%-38%), were purchased from Adamas-beta.

Synthesis of C₅H₇N₂ICl₄.

The ingredients comprised 4-aminopyridine (10 mmol, 941 mg), HIO₃ (20 mmol, 3518.2 mg), and HCl (2.5 ml) were put into water (31 ml). These materials were placed in beaker (50 ml), stirred for one hour at normal temperature. Subsequently, the beaker was placed in a fume hood and allowed to evaporate naturally at room temperature. Yellow needle-like crystals began to precipitate after approximately 1–2 weeks. The final yield was approximately 75%. Energy-dispersive X-ray spectroscopy demonstrated the presence of both iodine (I) and chlorine (Cl) elements in this crystal.

Single-crystal Structure Determination

Single-crystal X-ray diffraction data of compound C₅H₇N₂ICl₄ was collected on a Bruker APEX- II CCD diffractometer equipped with Mo K α radiation ($\lambda = 0.71073 \text{ \AA}$) at 293 K. Data reduction was accomplished with CrysAlisPro, and absorption correction based on the multi-scan method was applied.^[1] The structure was solved with the ShelXT 2014/5 solution program using Intrinsic Phasing methods and by utilizing Olex 2 as the graphical interface.^[2] The structure was refined with ShelXL 2018/3 using full matrix least squares minimization on F^2 .^[3] All of the non-hydrogen atoms were refined anisotropically. The H atoms were located at geometrically calculated positions and refined with isotropic thermal parameters. The structure was checked for missing symmetry elements using PLATON, and none was found.^[4]

Computational method

Both of the polarizability anisotropy and HOMO-LUMO gaps were calculated using Gaussian 09 at the B3LYP/LanL2DZ level and analyzed with Multiwfn^[7]. Calculations of electronic structure and optical property for C₅H₇N₂ICl₄ was performed utilizing CASTEP based on density function theory (DFT).^[5] Norm-conserving pseudopotential was used to treat the electron-core interactions, and GGA-PBE was chosen as exchange-correlation function.^[6] For crystal C₅H₇N₂ICl₄, the following orbital electrons were treated as valence electrons: I-5s²5p⁵, Cl-3s²3p⁵, C-2s²2p², N-2s²2p³, and H-1s¹. The numbers of plane waves included in the basis sets were determined by a cutoff energy of 750 eV. Monkhorst-Pack k-point sampling of 6 × 2 × 2 was applied to perform numerical integration of Brillouin zone for crystal **2**. During the optical property calculations, more than 2 times of valence bands for C₅H₇N₂ICl₄ were applied to ensure the convergence of linear optical property.

Table S1. Crystallographic Data and Structure Refinement Details for C₅H₇N₂Cl₄.

Empirical formula	C ₅ H ₇ N ₂ Cl ₄
Formula weight	363.83
Temperature/K	293(2)
Crystal system	Monoclinic
Space group	<i>P</i> 2 ₁ / <i>m</i>
<i>a</i> /Å	4.0937(5)
<i>b</i> /Å	11.9204(15)
<i>c</i> /Å	11.0250(16)
α /°	90
β /°	93.656(11)
γ /°	90
<i>V</i> /Å ³	536.91(12)
<i>Z</i>	2
ρ_{CALC} /cm ³	2.250
μ /mm ⁻¹	3.927
<i>F</i> (000)	344.0
Goodness-of-fit on <i>F</i> ²	1.076
Final <i>R</i> indexes [<i>I</i> ≥ 2σ (<i>I</i>)]	<i>R</i> ₁ = 0.0364, <i>wR</i> ₂ = 0.0812
Final <i>R</i> indexes [all data]	<i>R</i> ₁ = 0.0482, <i>wR</i> ₂ = 0.0885
Largest diff. Peak/hole / e Å ⁻³	1.14/-0.94

^a $R_1 = \frac{\sum ||F_o| - |F_c||}{\sum |F_o|}$; and $wR_2 = \left\{ \frac{\sum [w(F_o^2 - F_c^2)^2]}{\sum [w(F_o^2)^2]} \right\}^{1/2}$.

Table S2. Bond Lengths and Bond Angles for crystal C₅H₇N₂Cl₄.

Atom	Atom	Length/Å	Atom	Atom	Atom	Angle/°
I1	Cl1	2.4984(12)	Cl1	I1	Cl1 ¹	87.54(6)
I1	Cl1 ¹	2.4985(12)	Cl1	I1	Cl2	89.71(4)
I1	Cl2 ¹	2.5074(12)	Cl1 ¹	I1	Cl2	177.25(4)
I1	Cl2	2.5074(12)	Cl1 ¹	I1	Cl2 ¹	89.71(4)
N1	C1 ¹	1.354(6)	Cl1	I1	Cl2 ¹	177.25(4)
N1	C1	1.354(6)	Cl2 ¹	I1	Cl2	93.04(6)
N2	C3	1.297(9)	C1	N1	C1 ¹	122.1(7)
C1	C2	1.366(7)	N1	C1	C2	120.3(5)
C2	C3	1.421(6)	C1	C2	C3	119.7(5)
			N2	C3	C2	121.1(3)
			N2	C3	C2 ¹	121.1(3)
			C2 ¹	C3	C2	117.9(7)

Symmetry codes for the generated atoms : 1 +X,1/2-Y, +Z

Table S3. Hydrogen Bond Lengths (Å) and Bond Angles (°) in C₅H₇N₂I₄.

D	H	A	d(D-H)/Å	d(H-A)/Å	d(D-A)/Å	D-H-A/°
N1	H1	Cl1	0.86	2.70	3.404(6)	140.2
N2	H2	Cl2	0.89	2.66	3.404(5)	142.9

Table S4. Assignments of Additional Absorption Peaks in the IR Spectra of C₅H₇N₂I₄.

C ₅ H ₇ N ₂ I ₄	Assignments
3460-3220 cm ⁻¹	N-H stretching bands
3220-2930 cm ⁻¹	C-H stretching bands
1662-1480 cm ⁻¹	C-C and C-N stretching bands
1480-1350 cm ⁻¹	N-H in-plane bending bands
1350-1180 cm ⁻¹	C-H in-plane bending bands
1180-1000 cm ⁻¹	N-H out-plane bending bands
1000-890 cm ⁻¹	C-H out-plane bending bands
890-650 cm ⁻¹	I-Cl stretching bands
650-400 cm ⁻¹	I-Cl bending bands

The IR transparency from about 0.37 to 6 μm

Table S5. Comparisons of the Optical Property of Compound containing [IO₃]⁻ group.

Compound	Δn @546nm	Bandgap	Reference
C ₅ H ₇ N ₂ Cl ₄	0.94	2.29	This work
(C ₅ H _{6.16} N ₂ Cl _{0.84})(IO ₂ Cl ₂)	0.67	3.38	[8]
(C(NH ₂) ₃) ₂ (I ₂ O ₅ F)(IO ₃)(H ₂ O)	0.068	4.49	[9]
C(NH ₂) ₃ IO ₂ F ₂	0.11	4.81	[9]
Ce(IO ₃) ₃ F	0.225	2.55	[10]
SrTi(IO ₃) ₆ ·2H ₂ O	0.093	2.5	[11]
(H ₃ O) ₂ Ti(IO ₃) ₆	0.045	2.62	[12]
SrSn(IO ₃) ₆	0.116	3.19	[11]
[Al(H ₂ O) ₆](IO ₃) ₂ (NO ₃)	0.253	3.33	[13]
Ce(IO ₃) ₂ (NO ₃)	0.039	3.14	[10]
C(NH ₂) ₃ MoO ₃ (IO ₃)	0.426	3.33	[14]
(C ₇ H ₄ NO ₄)(IO ₃)	0.35	4.12	[15]
Rb ₂ MoO ₂ (I ₂ O ₆)(IO ₃) ₂	0.261	3.22	[14]
C(NH ₂) ₃ IO ₃	0.075	4.57	[9]
K ₂ Na(I ₃ O ₈) ₃	0.283	3.89	[16]
HfF ₂ (IO ₃) ₂	0.333	4.11	[17]
Na ₂ [B ₄ IO ₉](IO ₃)	0.298	4.3	[18]
Sc(IO ₃) ₂ (NO ₃)	0.348	4.15	[19]

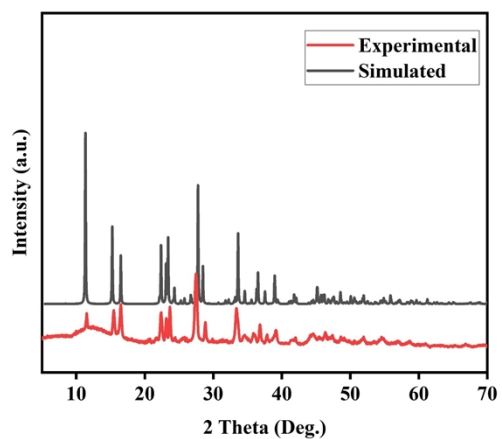


Figure S1. The powder X-ray diffraction analysis of $C_5H_7N_2ICl_4$.

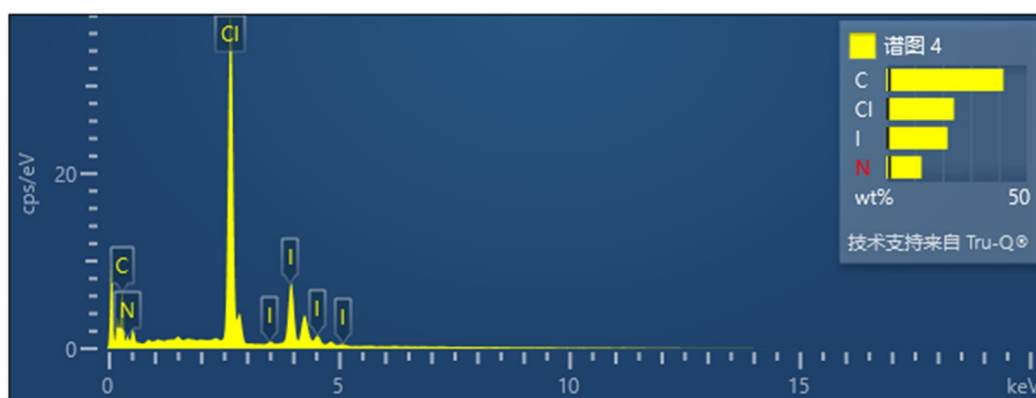


Figure S2. The energy-dispersive X-ray spectroscopy of $C_5H_7N_2ICl_4$.

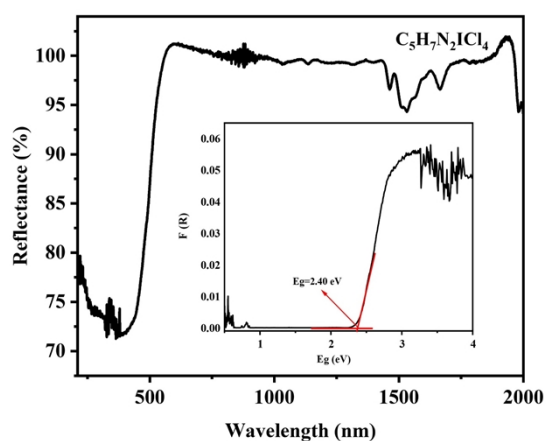


Figure S3. The UV-vis-NIR diffuse reflectance spectrum and experimental bandgap of $C_5H_7N_2ICl_4$.

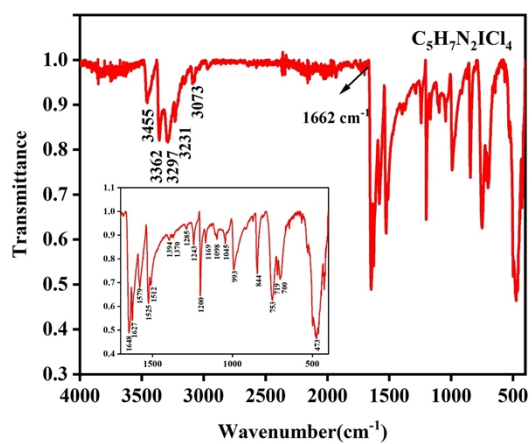


Figure S4. The infrared (IR) spectrum of $C_5H_7N_2ICl_4$.

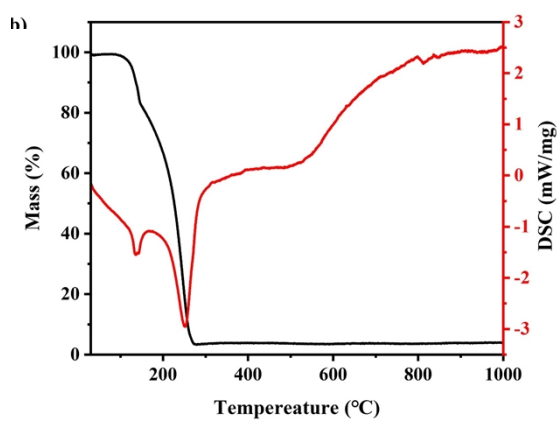


Figure S5. TG and DSC curves of $C_5H_7N_2ICl_4$.

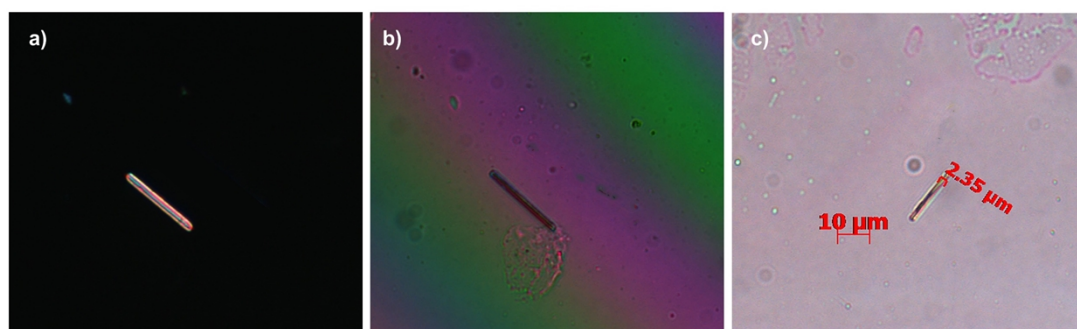


Figure S6. (a) the original $C_5H_7N_2ICl_4$ under the cross-polarized light; (b) $C_5H_7N_2ICl_4$ achieving complete extinction; (c) the thickness of $C_5H_7N_2ICl_4$ used for birefringence measurement.

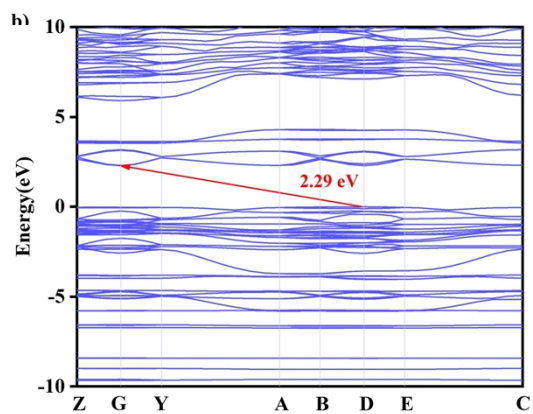


Figure S7. Band structure of $C_5H_7N_2I_4$.

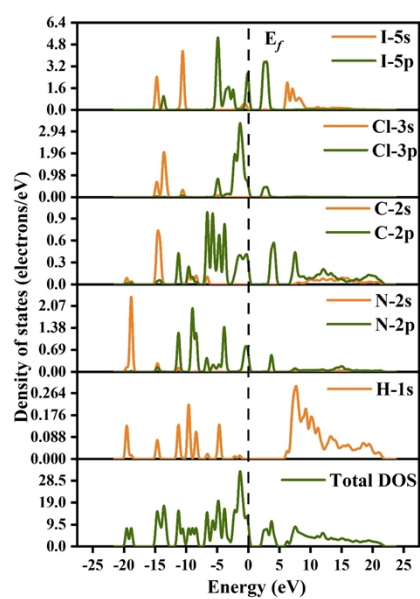


Figure S8. PDOS and TDOS diagrams for $C_5H_7N_2I_4$.

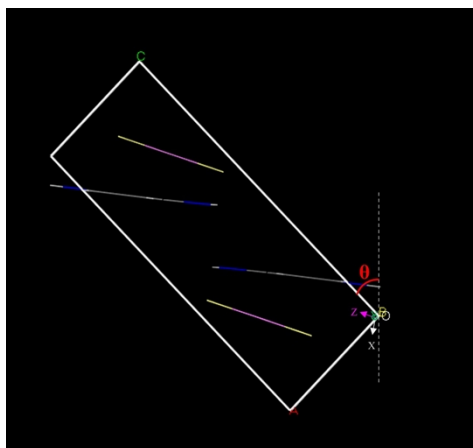


Figure S9. Distribution of the rotated ac plane and diagonalized dielectric tensor axes of $C_5H_7N_2ICl_4$.

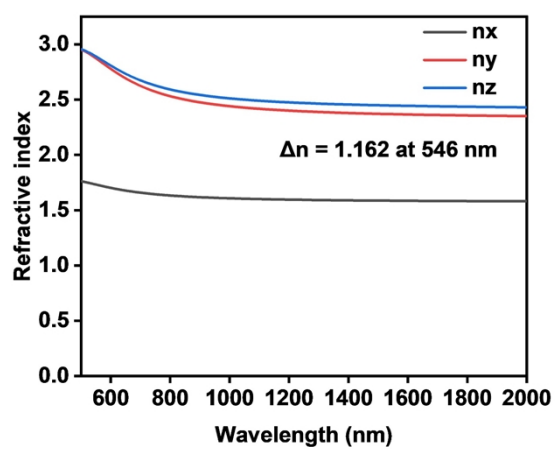


Figure S10. Refractive index and calculated birefringence of $C_5H_7N_2ICl_4$.

References

- [1] R. H. Blessing, *Acta Crystallogr A* **1995**, *51* (Pt 1), 33-38.
- [2] a) G. M. Sheldrick, *Acta Crystallographica Section A* **2015**, *71*, 3-8; b) O. V. Dolomanov, L. J. Bourhis, R. J. Gildea, J. A. K. Howard, H. Puschmann, *Journal of Applied Crystallography* **2009**, *42*, 339-341.
- [3] G. M. Sheldrick, *Acta Crystallogr C Struct Chem* **2015**, *71*, 3-8.
- [4] A. L. Spek, *Journal of Applied Crystallography* **2003**, *36*, 7-13.
- [5] a) V. Milman, B. Winkler, J. A. White, C. J. Pickard, M. C. Payne, E. V. Akhmatkaya, R. H. Nobes, *International Journal of Quantum Chemistry* **2000**, *77*, 895-910; b) S. J. Clark, M. D. Segall, C. J. Pickard, P. J. Hasnip, M. I. J. Probert, K. Refson, M. C. Payne, *Zeitschrift für Kristallographie - Crystalline Materials* **2005**, *220*, 567-570.
- [6] a) J. P. Perdew, K. Burke, M. Ernzerhof, *Physical Review Letters* **1996**, *77*, 3865-3868; b) J. S. Lin, A. Qteish, M. C. Payne, V. V. Heine, *Phys Rev B Condens Matter* **1993**, *47*, 4174-4180.
- [7] T. Lu, F. Chen, *Journal of Computational Chemistry* **2012**, *33*, 580-592.
- [8] Q.-Q. Chen, C.-L. Hu, M.-Z. Zhang, J.-G. Mao, *Chemical Science* **2023**, *14*, 14302-14307.
- [9] J. Cui, S. Wang, A. Tudi, M. Gai, Z. Yang, S. Pan, *Inorg. Chem.* **2024**, *63*, 661-667.
- [10] N. Ma, Y. Huang, C.-L. Hu, M.-Z. Zhang, B.-X. Li, J.-G. Mao, *Inorg. Chem.* **2023**, *62*, 15329-15333.
- [11] K. Liu, J. Han, J. Huang, Z. Wei, Z. Yang, S. Pan, *RSC Advances* **2021**, *11*, 10309-10315.
- [12] Y.-B. Fang, R.-B. Fu, H.-X. Tang, Q.-R. Shui, Z.-J. Ma, X.-T. Wu, *Inorg. Chem.* **2021**, *60*, 5821-5828.
- [13] Z. Bai, C.-L. Hu, D. Wang, L. Liu, L. Zhang, Y. Huang, F. Yuan, Z. Lin, *Chemical Communications* **2020**, *56*, 11629-11632.
- [14] W. Zeng, Y. Tian, X. Dong, L. Huang, H. Zeng, Z. Lin, G. Zou, *Chemistry of Materials* **2024**, *36*, 2138-2146.
- [15] M.-B. Xu, Q.-Q. Chen, B.-X. Li, K.-Z. Du, J. Chen, *Chinese Chemical Letters* **2024**, *36*, 110513.
- [16] M.-Q. Lin, M.-F. Duan, J.-G. Mao, B.-P. Yang, *New Journal of Chemistry* **2025**, *49*, 6103-6108.
- [17] Y. Huang, Z. Fang, B.-P. Yang, X.-Y. Zhang, J.-G. Mao, *Scripta Materialia* **2023**, *223*, 115082.
- [18] Y.-L. Deng, C.-L. Hu, X. Xu, M.-Z. Zhang, J.-G. Mao, *J. Am. Chem. Soc.* **2025**, *147*, 12858-12865.
- [19] C. Wu, X. Jiang, Z. Wang, L. Lin, Z. Lin, Z. Huang, X. Long, M. G. Humphrey, C. Zhang, *Angewandte Chemie International Edition* **2021**, *60*, 3464-3468.